

# TRIBOLOGICAL BEHAVIOR OF ABS-LIKE PHOTOPOLYMER RESINS IN SLIDING BEARINGS MANUFACTURED BY DLP PRINTING

Gheorghe Macovei<sup>1</sup>, Dragoș Luca<sup>1</sup>, George Popa<sup>1</sup>, Viorel Paleu<sup>1\*</sup>

<sup>1</sup>“Gheorghe Asachi” Technical University of Iași, Mechanical Engineering, Mechatronics and Robotics Department, Mechanical Engineering Faculty, 43 Prof. D. Mangeron Blvd. 700050, Iasi, Romania, [gheorghe.macovei@student.tuiasi.ro](mailto:gheorghe.macovei@student.tuiasi.ro), [viorel.paleu@academic.tuiasi.ro](mailto:viorel.paleu@academic.tuiasi.ro)

**Abstract:** *Abstract: The 3D printing technology that uses photopolymerization, widely known among hobbyists under the acronym DLP (digital light processing), has the potential to revolutionize the manufacturing of sliding bearings used for light loads and in remote environments, where the availability of spare parts is problematic. In order to understand how these materials behave when subjected to friction and wear, studies are needed, as the current state of knowledge is insufficient. This article presents the behavior of multiple samples, manufactured under different parameters, and subjected to different loads and different speeds of contact. These samples were also subjected to UV curing. The tests showed correlation with other articles from literature.*

**Keywords:** *additive manufacturing, digital light processing, tribology, friction, denting*

## 1. Introduction

Sliding bearings are critical elements in any mechanical system, transferring the normal load to the adjacent component, and allowing the movement in other directions, ideally, with zero energy loss.

In practical terms, approximately one-third of available energy and 5% of global wealth are wasted in the friction process, in various systems, through the conversion of huge amounts of useful energy into useless heat [Yu, 2021].

The bearing interface is subjected to friction and wear, which over time will cause the joint to fail. This is a well-known fact, which is why car and machinery manufacturers are required by law to ensure that spare parts are available on the market for a certain number of years after the end of production.

The European Union has regulated this through EU 2024/1799, which specifies that the manufacturers must make available the spare parts, tools, and technical information (manuals, diagnostic software, etc.) necessary

to repair goods covered by the repairability requirements [Document 32024L1799].

These parts/tools must be offered at a reasonable price so that access to them is not discouraged.

However, there are countless cases where spare parts are unavailable, not because they do not exist, but for other reasons, such as: the cost of delivery of the part does not justify the investment, the delivery time is too long, political reasons, sanctions, conflict or war, etc.

In all these cases, in order to keep the mechanical system operational, an alternative must be found to procure the necessary component. One method is the manufacturing on-site.

For the case of polymer-based bearings, a well-known manufacturing method that does not require dedicated tooling, is 3D printing through digital light processing (DLP).

The DLP printing uses photosensitive resin, which is polymerized layer by layer until the entire component is printed.

In recent years, the study of the tribological behavior of components manufactured using

digital light processing has begun to attract the attentions of academics.

Muammal et al. [Muammal, 2020] has studied the impact of curing process with UV light and concluded that the uncured samples showed the greatest wear depth and the lowest friction coefficient compared to the samples that were cured.

Kazemi et al. [Kazemi, 2020] conducted an investigation into the abrasion behavior of components fabricated via Digital Light Processing (DLP) using a pin-on-disk tribometer. In their experiments, neither the pin nor the disk was post-cured with UV light. A key variable was the orientation of the pin, which was tested at various angles. Their results demonstrated that normal load exerted on the pin is the primary determinant of the abrasion rate, accounting for approximately 71.58% of the influence. The angle of the surface normal relative to the load contributes about 27.70%, while layer thickness has a negligible effect, at about 0.11%.

Existing literature on the tribological behavior of DLP-printed specimens under low load and in dry conditions is limited, particularly with regard to ball-on-plate configurations.

In order to address this gap and achieve a more comprehensive tribological characterization of DLP-printed materials, the present study investigates the effect of UV post-curing. The article presents the results of friction and denting tests, and compares continuous circular motion tests with linear reciprocating motion tests.

## 2. Materials and equipment

### 2.1 Materials.

The specimens were fabricated using a white resin produced by Anycubic that was specifically developed for use with Digital Light Processing (DLP) 3D printing technology. The parameters of the resin are presented in Table 1.

This material is designed to produce high-resolution outputs with superior accuracy and fine detail reproduction. It consists of a photosensitive liquid polymer that solidifies when exposed to light of specific wavelengths.

Anycubic's white resin is characterized by its excellent flow properties, which enable uniform distribution within complex geometries and ensure accurate replication of intricate features with minimal surface defects.

Table 1

Parameters of Anycubic White resin [5]

Parameter	Value	Parameter	Value
Viscosity (mPa×s) 25°C	150-200	Density $g/cm^3$	1.05-1.25
Wavelength (nm)	405	Hardness (Shore D)	80D
Tensile strength (MPa)	36-45	Elongation (%)	8-12
Flexural strength (MPa)	50-65	Flexural modulus (MPa)	1200-1600
Volumetric shrinkage (%)	4.5-5.5	Notched impact strength (J/m)	25
Heat deflection temperature (°C)	65-70	Shelf life (year)	1

The material also demonstrates high dimensional stability throughout the printing process, significantly reducing the likelihood of warping or deformation and enhancing the overall precision and consistency of the printed components [5].

The sample is designed in the form of a disc to facilitate attachment to the tribometer (figure 1).

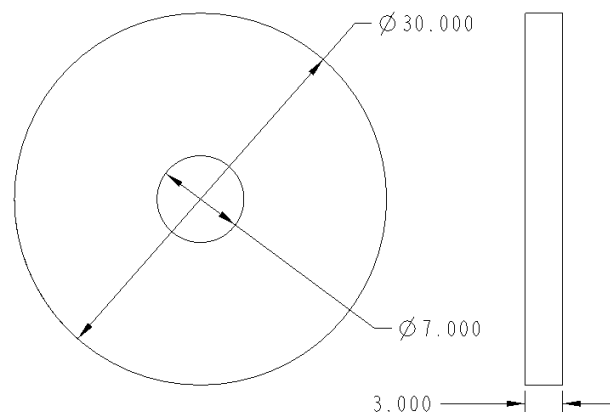


Figure.1 Mechanical dimensions of the tested specimens (all dimensions in millimeters).

The counterpart employed in all tribological experiments is a bearing steel sphere with a diameter of 6.35 mm.

## 2.2 Equipment

In this study, the experimental setup comprises a resin 3D printer, a UV curing chamber, a surface roughness measurement instrument, and a tribometer.

The resin specimens were produced using the printer Anycubic Photon Mono 4K, which is a high-resolution resin 3D printer designed for precision and efficiency. Equipped with a 6.23-inch monochrome LCD screen boasting a  $3840 \times 2400$ -pixel (4K) resolution, it delivers over 9.2 million pixels, providing detailed and sharp prints. The printer features a build volume of  $165 \times 132 \times 80$  mm, suitable for a variety of model sizes. Its 15-LED parallel matrix light source ensures uniform exposure, with a light transmittance of 7% and a contrast ratio of 400:1, enhancing print quality.

With a horizontal resolution of  $35 \mu\text{m}$  and a printing speed of up to 50 mm/h, it offers both fine detail and efficiency. The printer operates with a 45W power supply and is controlled via a 2.8-inch TFT touch screen. It supports 405nm UV resins and comes with the Photon Workshop software for slicing. The machine dimensions are  $383 \times 227 \times 222$  mm, and it weighs 4.3 kg. [6].

The UV curing chamber is The Wanhao Boxman-1, which is a UV LED curing chamber designed to post-process resin 3D prints from SLA, DLP, and LCD printers, enhancing their mechanical properties and surface finish. It features four strategically positioned 405 nm UV LED arrays that provide uniform exposure from all sides, ensuring consistent curing of models up to  $32 \times 20 \times 20$  cm in size. The chamber is equipped with a mirrored interior and a transparent glass platform, allowing for multi-tier curing setups. With a power output of 120 W and a voltage range of 110–220 V, it is suitable for global use. The Boxman-1 includes a  $57.6 \times 43.2$  mm touch LCD screen for easy operation and an  $85 \times 85 \times 10$  mm fan for effective ventilation [7].

The tribometer CETR UMT-2 (figure 2) is a versatile tool designed for comprehensive

tribological testing across various materials and conditions. It offers both reciprocating and unidirectional sliding modes, accommodating loads ranging from 0.01 N to 200 N, with frequencies up to 40 Hz and sliding speeds from 0.01 m/s to 10 m/s. The system supports stroke lengths between 1 mm and 25 mm in reciprocating mode [User's Manual, 2004].

## 3. Printing, curing and testing parameters

### 3.1 Printing parameters

The parameters used for fabricating the samples are detailed in Figure 2.

Layers Thickness(mm)	0.050
Normal Exposure Time(s)	8.000
Off Time(s)	0.500
Bottom Exposure Time(s)	40.000
Bottom Layers	6
Anti-alias	1
Use Random Erode Shell	<input type="checkbox"/>
Control Type	Basic
Z Lift Distance(mm)	6.000
Z Lift Speed(mm/s)	4.000
Z Retract Speed(mm/s)	6.000

Figure.2 Printing parameters of the samples.

One of the critical variables for our investigation is the layer height, set at  $50 \mu\text{m}$ , along with the standard exposure duration per layer, which for this work is 8 seconds.

### 3.2 Curing parameters

The specimens were cured for different durations in order to assess the effect on their tribological properties. Samples denoted S1 through S5 underwent curing as detailed in Table 1.

Table 2

The curing plan of the tested samples.

	S1	S2	S3	S4	S5
UV time [s]	0	3	4	5	20

### 3.3 Testing parameters

All specimens underwent the same environmental and preparatory conditions and were tested under controlled tribological setups to allow direct comparison of reciprocating linear motion versus continuous circular sliding. In the reciprocating linear tests (figure 3), the ball executed a 10 mm back-and-forth stroke across the specimen at 5 mm/s under a normal load of 10 N for 600 seconds—this corresponds to 150 cycles and a total sliding distance of 3,000 mm, with each test repeated three times.

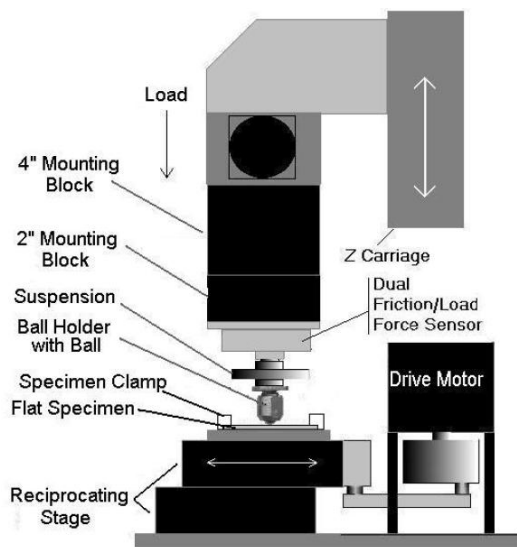


Figure.3 Simplified view of the testing system used for linear motion.

Additionally, a scratch test was carried out under 5 N at 0.167 mm/s over 60 seconds along a 10 mm path, while a denting (indentation) test used a Rockwell diamond tip of 200  $\mu\text{m}$  radius, following a predefined profile.

By holding constant the normal force and contact geometry but varying motion type, sliding path, cycle reversals, and test duration, the comparison isolates the effects of motion

mode on friction, wear rates, and surface deformation.

The denting test was carried out in accordance with the profile depicted in figure 4, utilizing a Rockwell diamond tip with a radius of 200  $\mu\text{m}$ .

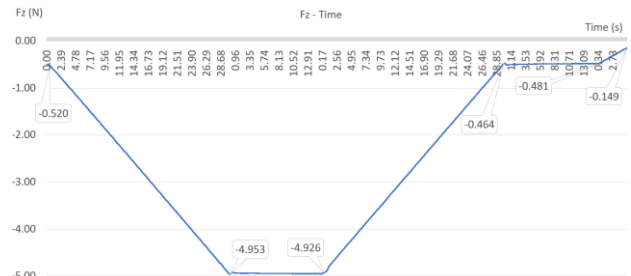


Figure.4 The profile of the normal load applied for the denting test

In contrast, circular sliding tests were performed with the ball sliding over a rotating disc (figure 5) of 10 mm radius at 1,000 rpm, under the same 10 N normal load, but for a shorter duration of 300 seconds.

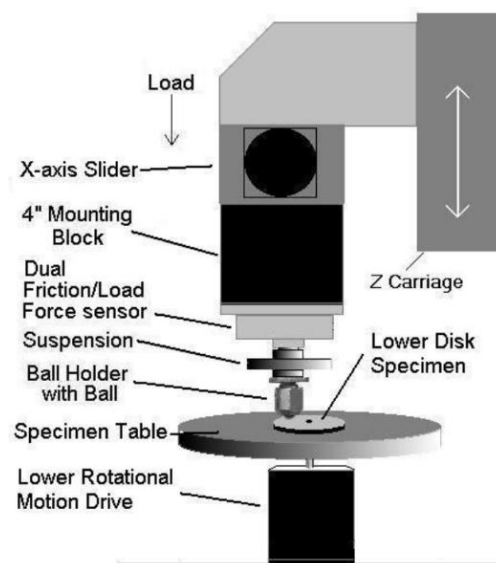


Figure.5 Simplified view of the testing system used for circular motion.

## 4 Results and discussions

### 4.1 Coefficient of friction (COF) and its evolution

#### 4.1.1 Continuous rotational movement

For samples manufactured using DLP technology that were subjected to the rotation



test (figure 6), the COF evolved in two distinct stages: an initial running-in period involving a rapid increase in COF, followed by a stabilization phase. The average COF values obtained ranged from approximately 0.39 to 0.49, depending on the UV exposure time.

Samples treated with UV light for 20 seconds exhibited the lowest COF values (approximately 0.39), indicating more complete polymerization and superior hardness. After stabilization, a slow but steady increase in COF was observed, probably due to local degradation or interlayer heating.

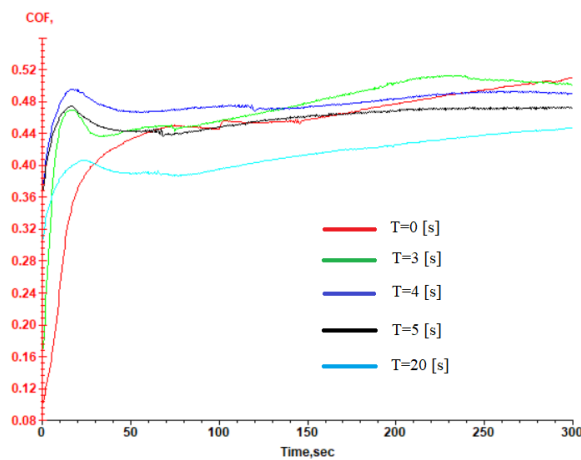


Figure.6 The variation of COF in time for circular motion

#### 4.1.2 Reciprocating motion

In reciprocating tests (figure 7), the COF behavior also followed two phases: running-in and stabilization. The average COF values seem to be significantly lower than for rotational motion, ranging from ~0.056 to 0.092 (in the stabilization phase). Samples exposed to UV for 20 seconds achieved the lowest coefficient (~0.058).

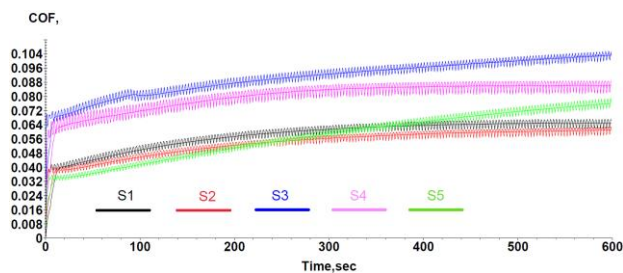


Figure.7 The variation of COF in time for linear motion

The COF evolved more stably over time than in rotation, with moderate ascending

variations, suggesting a balance between stress relaxation and mechanical degradation.

The undulatory characteristic reflects the fluctuations in the coefficient of friction along the wear path — in other words, variations caused by the reciprocating motion during the test.

#### 4.1.2 Comparison of the two configurations

The COFs obtained for reciprocating motion are almost an order of magnitude smaller than those obtained for rotational motion. This difference can be attributed to the much lower contact speed and reduced contact duration between alternating cycles, as well as heat dissipation phenomena. In both configurations, a longer UV treatment time (20 seconds) results in lower COF values, supporting the hypothesis that a higher degree of polymerization reduces friction.

Myshkin et al. [Myshkin, 2009] determined that in polymers, the friction force is significantly influenced by the applied load, the sliding speed, and both the ambient and contact temperature.

## 4.2 Wear and denting

### 4.2.1 Observations on wear

Optical examination of the surfaces worn during the rotation tests revealed fine marks with no obvious deep grooves. The roughness of the contact area increased after the test, particularly for samples with lower UV exposure.

In reciprocating motion tests, samples that had been subjected to UV treatment exhibited uniform wear without the formation of chips.

### 4.2.2 Denting tests

The denting tests (figure 8) reveal the impact of UV curing duration on the hardness of the samples, with the specimen cured for 20 seconds exhibiting the highest hardness.

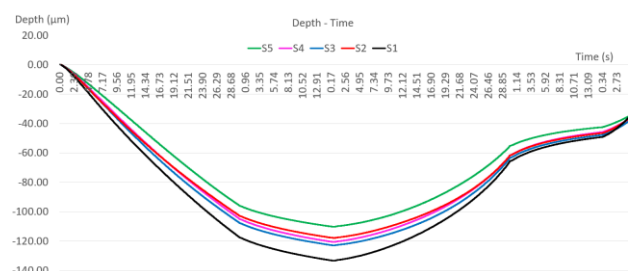


Figure.8 The variation of the denting depth during testing

The hardness and Young's modulus values are presented in Table 3.

Table 3  
The Rockwell hardness and the Young modulus of the unaged samples.

	S1	S2	S3	S4	S5
Hardness [GPa]	0.025	0.029	0.027	0.028	0.033
Young Modulus [GPa]	0.222	0.309	0.289	0.288	0.32

#### 4.2.3 Correlations between wear hardness and COF

Increased material hardness, as a result of adequate UV exposure, directly contributes to a lower COF and reduced wear. In reciprocating motion, elastic behavior and intermittent contact mitigate continuous degradation compared to rotational motion.

Post-curing UV treatment significantly enhances the mechanical properties, including hardness, of samples produced via DLP additive manufacturing.

Studies indicate that the post-polymerization (post-curing) process, often involving UV light, directly leads to an increase in the microhardness value of 3D-printed resin samples [Büyükpolat, 2025]. The post-treatment is essential for finalizing the polymerization process, thereby enhancing the overall material properties [Perin, 2023].

In addition to hardness, UV post-curing is a commonly utilized technique to alter and enhance the stiffness and strength of materials. This is accomplished by ensuring complete polymerization of any uncured resin within the printed component [Perin, 2023].

The effectiveness of UV treatment on hardness and other mechanical properties is influenced by several parameters, including post-polymerization time and the type of curing device employed [Büyükpolat, 2025]. Research on stereolithography, which shares photopolymerization principles with DLP, has examined the impact of layer exposure time

during UV curing on Brinell hardness [Pszczółkowski, 2025].

Besides bulk hardness, UV post-curing may affect surface characteristics. Post-processing using heating and UV light results in reduced wear depth for DLP printed specimens, indicating enhanced surface durability [Hanon, 2020].

The broader context of post-curing methods in photopolymerization-based additive manufacturing, including SLA and its comparison to DLP, examines their effects on ultimate tensile strength, hardness, dimensional variations, and surface roughness. Various post-curing processes, such as UV chambers, can produce differing effects on the performance of the final part [Zhao, 2020].

In conclusion, UV treatment is an essential process in the DLP additive manufacturing workflow, enhancing the hardness and mechanical performance of printed components. Optimizing the parameters of the post-curing process is crucial for attaining the desired material properties.

## 5 Conclusions

Combining the results of both test setups, we can draw conclusions regarding the influence of the type of movement and UV treatment on the tribological properties of DLP materials:

The effect of UV treatment is fundamental: longer exposure (20 s) leads to lower COF values and higher hardness in both tested configurations.

The tribological configuration strongly influences the magnitude of the COF: reciprocating motion produces significantly lower values than continuous rotation, due to more favorable dissipation and relaxation conditions.

The wear pattern differs: in rotation, fine particles and increased roughness appear, while in reciprocating motion, wear is more uniform and less destructive.

From an application point of view, for tribological components operating in reciprocating mode, appropriately UV-treated

DLP materials can ensure low COF and long-lasting performance.

#### 4 References

- [Yu, 2021] Yu Z., Hui, M., Peng, C. Chao C., Laifei C., and Konstantinos G. D. *ACS Nano* **2021**
- Document 32024L1799, <https://eur-lex.europa.eu/legal-content/ro/ALL/?uri=CELEX:32024L1799>
- [Muammel, 2020] Muammel M. H., László Z., *Tribological and mechanical properties investigation of 3D printed polymers using DLP technique.* <https://doi.org/10.1063/5.0000267>
- [Kazemi, 2020] Kazemi, M., Rahimi, A., *An experimental and theoretical study of the abrasion performance of digital light processing parts.* [doi:10.1177/0954405420981333](https://doi.org/10.1177/0954405420981333)
- <https://store.anycubic.com/products/anycubic-abs-like-resin>
- <https://store.anycubic.com/products/photon-mono-4k>
- <https://the3dprinterstore.com/products/wanhao-uv-curing-box>
- [User's Manual, 2004] User's Manual, CETR *UMT-2 Multi-Specimen Test System*, Version 1.01, 09/29/04.
- [Myshkin, 2009] Myshkin, N., and Kovalev, V., *Adhesion and friction on polymers.* 2009 [doi:10.1142/9781848162044\\_0001](https://doi.org/10.1142/9781848162044_0001)
- [Büyükpolat, 2025] Büyükpolat, M., Çal, İ. K., Eryılmaz, B., Ersöz, B., Aydın, N., and Karaoğlu, S., *Mechanical and optical effects of post-curing time and device type in two 3D-printed resin systems.*, *BMC Oral Health*, 25(1), 1401, 2025. <https://doi.org/10.1186/s12903-025-06813-6>
- [Hanon, 2020] Hanon, M. M. and Zsidai, L., *Tribological and mechanical properties investigation of 3D printed polymers using DLP technique.*, *AIP Conference Proceedings*, 2020. <https://doi.org/10.1063/5.0000267>
- [Perin, 2023] Perin, M., Quagliato, L., Berti, G., Jang, C., Jang, S., and Lee, T., *Manufacturing Process, Tensile-Compressive, and Impact Properties of Tungsten (W)-Particle-Reinforced SLA Methacrylate.*, *Polymers*, 15(24), 4728, 2023. <https://doi.org/10.3390/polym15244728>
- [Pszczółkowski, 2025] Pszczółkowski, B. and Zaborowska, M., *Effect of Layer Exposure Time in SLA-LCD Printing on Surface Topography, Hardness and Chemical Structure of UV-Cured Photopolymer.*, *Lubricants*, 13(9), 406, 2025. <https://doi.org/10.3390/lubricants13090406>
- [Zhao, 2020] Zhao, J., Yang, Y. and Li, L., *A comprehensive evaluation for different post-curing methods used in stereolithography additive manufacturing.*, *Journal of Manufacturing Processes*, 56, 867, 2020. <https://doi.org/10.1016/j.jmapro.2020.04.077>